50. van de Wetering,M., Sancho,E., Verweij,C. *et al.* (2002) The beta-catenin/TCF-4 complex imposes a crypt progenitor phenotype on colorectal cancer cells. *Cell*, **111**, 241–250.
51. Korinek,V., Barker,N., Moerer,P., van Donselaar,E., Huls,G., Peters,P.J. and Clevers,H. (1998) Depletion of epithelial stem-cell compartments in the small intestine of mice lacking Tcf-4. *Nature Genet.*, **19**, 379–383.
52. Sheng,H., Shao,J., Williams,C.S., Pereira,M.A., Taketo,M.M., Oshima,M., Reynolds,A.B., Washington,M.K., DuBois,R.N. and Beauchamp,R.D. (1998) Nuclear translocation of β-catenin in hereditary and carcinogen-induced intestinal adenomas. *Carcinogenesis*, **19**, 543–549.
53. Takahashi,M., Nakatsugi,S., Sugimura,T. and Wakabayashi,K. (2000) Frequent mutations of the β-catenin gene in mouse colon tumors induced by azoxymethane. *Carcinogenesis*, **21**, 1117–1120.
54. Kielman,M.F., Rindapaa,M., Gaspar,C., van Poppel,N., Breukel,C., van Leeuwen,S., Taketo,M.M., Roberts,S., Smits,R. and Fodde,R. (2002) Apc modulates embryonic stem-cell differentiation by controlling the dosage of β-catenin signaling. *Nature Genet.*, **32**, 594–605.

Received October 24, 2003; revised March 11, 2004; accepted March 22, 2004

Myxoid Epithelioid Gastrointestinal Stromal Tumor (GIST) With Mast Cell Infiltrations: A Subtype of GIST With Mutations of Platelet-Derived Growth Factor Receptor Alpha Gene

SHINJI SAKURAI, MD, TADASHI HASEGAWA, YUJI SAKUMA, YUTAKA TAKAZAWA, ATSUSHI MOTEGI, TAKASHI NAKAJIMA, KEN SAITO, MASASHI FUKAYAMA, AND TADAKAZU SHIMODA

We analyzed 30 gastrointestinal stromal tumors (GISTs) that were immunohistochemically weak or negative for KIT. Histologically, all 30 GISTs consisted of epithelioid tumor cells in at least a part of the tumor. The tumor cells showed different morphologies and arranged themselves in different histological patterns. In 20 of the 30 GISTs, round or oval epithelioid tumor cells often showed a less cohesive pattern of growth and showed eosinophilic cytoplasm and peripherally placed nuclei with myxoid stroma, whereas in the remaining 10 cases, tumor cells were arranged in a more cohesive pattern without myxoid stroma. The former type of tumors is called *myxoid epithelioid GISTs* in this study. Subsequent mutational analyses showed that the platelet-derived growth factor receptor alpha (*PDGFRA*) gene mutations in exon 12 or exon 18 were identified in 20 (66.7%) of the 30 GISTs, and especially in 18 (90%) of the 20 myxoid epithelioid GISTs. Moreover, 17 (85%) of the 20 myxoid epithelioid GISTs were accompanied by mast cell infiltrations within the tumor nodules. In the remaining cases, 2 (6.7%) of the 30 GISTs had c-*kit* gene mutations in exon 11, and no mutation was found in 8 (26.7%) of 30 GISTs. None of the patients with myxoid epithelioid GISTs died of disease. These results suggest that myxoid epithelioid GISTs are a distinct subtype of GISTs that are closely correlated with the *PDGFRA* gene mutation and that recognition of such histological characteristics should be helpful for molecular subclassification of GISTs that are important for molecular targeting therapy by imatinib mesylate (STI571). HUM PATHOL 35:1223-1230. © 2004 Elsevier Inc. All rights reserved.

Key words: **GISTs, myxoid epithelioid, mast cell infiltration, *PDGFRA* gene mutation.**

Abbreviations: **GISTs, gastrointestinal stromal tumors; PDGFRA, platelet-derived growth factor receptor alpha; ICCs, interstitial cells of Cajal; PCR, polymerase chain reaction.**

Gastrointestinal stromal tumors (GISTs) are the most frequent nonepithelial neoplasm in the stomach and intestine.[1-5] In the past, most GISTs were thought to originate from smooth muscle, based on their histological features. However, recent reports clarified the close relationship between GISTs and interstitial cells of Cajal (ICCs), which play important roles, such as as the pacemaker that enables cooperative peristalsis or as the mediator of nitric oxide–mediated transmission from nerve terminals to smooth muscle cells in the gastrointestinal tract.[6,7] Simultaneous expression of specific molecules such as KIT, CD34, the embryonic isoform of myosin heavy chain (SMemb), and nestin in both ICCs and GISTs[8-12] leads us to consider that GISTs may develop from ICCs or their progenitor cells. In previous reports, about 90% of GISTs were immunohistochemically positive for KIT,[8-12] and mutations of the c-*kit* gene have been found in most of these KIT-positive GISTs.[13] Recently, mutations of the platelet-derived growth factor receptor alpha (*PDGFRA*) gene encoding platelet-derived growth factorα have been reported in GISTs that are negative for c-*kit* gene mutations.[14,15]

Histopathologically, most GISTs consist of spindle tumor cells with acidophilic fibrillary cytoplasm and elongated or cigar-shaped nuclei with perinuclear vacuoles. In our experience, these typical GISTs are usually KIT positive by immunohistochemical staining. On the other hand, tumor cells show pleomorphic or epithelioid histology in rare cases of GISTs, and such histology is sometimes difficult for pathologists to diagnose. In such cases, an immunohistochemically positive result for KIT is a useful marker for the diagnosis of GISTs.

However, in our previous analyses, we found that KIT immunoreactivity in epithelioid cells of GISTs was weaker than in spindle cells in the same tissue sections or other tumors. Moreover, some GISTs were completely negative for KIT. Lack of the c-*kit* gene mutation had also been reported in GISTs with an epithelioid component.[16] In such cases, accuracy of the diagnosis of GISTs may be questionable. In this study, to clarify the clinicopathologic features and molecular genetic background of such tumors, we analyzed 27 cases of

From the Department of Pathology, Jichi Medical School, Tochigi, Department of Pathology, National Cancer Center Research Institute and Hospital, Tokyo, Department of Pathology, Graduate School of Medicine, University of Tokyo, Tokyo, and Department of Tumor Pathology, Gunma University Graduate School of Medicine, Maebashi, Gunma, Japan. Accepted for publication July 1, 2004.

Supported by a Grant-in-Aid for Scientific Research from the Ministry of Education, Science, Sports, and Culture of Japan and by a Grant-in-Aid for Cancer Research from the Ministry of Health, Labor and Welfare of Japan.

Address correspondence and reprint requests to Shinji Sakurai, MD, 3311-1 Yakushiji, Minamikawachi-machi, Kawachi-gun, Tochigi 329-0498, Japan.

0046-8177/$—see front matter

doi:10.1016/j.humpath.2004.07.008

TABLE 1. Risk Category for Gastrointestinal Stromal Tumor Based on the MIB-1 Grading System and Tumor Size

	Tumor size (cm)		
Grade*	≤5	<5-≤10	>10
Low	Low risk	Intermediate risk	High risk
High	High risk	High risk	High risk

*Low grade, MIB-1–labeling index of <10% and no tumor necrosis; high grade, MIB-1–labeling index of ≥10% or tumor necrosis.

GISTs showing weak or negative staining for KIT. From the results of histological findings and mutational analyses of the c-*kit* and the *PDGFRA* gene, we showed that specific histology of GISTs was closely correlated with the *PDGFRA* gene mutation and termed such GISTs *myxoid epithelioid GISTs*.

MATERIALS AND METHODS

KIT-Weak or KIT-Negative GISTs

The study was approved by the research ethics committee of Jichi Medical School. Of the 303 GISTs collected at Jichi Medical School Hospital, National Cancer Center Hospital, and related hospitals, all of which were analyzed by the immunohistochemical techniques described in this section, 30 (9.9%) primary GISTs showing negative or weak immunostaining for KIT were selected. A consensus judgment was adopted as the proper immunohistochemical score of the tumor on the basis of strength: 0, negative; 1+, weak staining; 2+, moderate staining; 3+, strong staining. Tissue mast cells, which stain 2+ or 3+, were used as internal positive controls for KIT. The distribution of positive cells was also recorded in an effort to impart the diffuse or focal nature of the positive cells: sporadic (positive cells <10%), focal (10% to <50% positive cells), or diffuse (50% positive cells). The immunohistochemical scores of 0 and 1+ with focal to diffuse distribution were considered to be KIT-weak or KIT-negative GISTs.

Of these, 29 GISTs were surgically resected from 29 patients, and the remaining 1 was from an autopsy case in which the patient died of hypoxic encephalopathy (case 22). The sites of the primary tumors were the stomach (n = 26), esophagus (n = 1), small intestine (n = 1), and omentum (n = 2). One patient (case 17) was treated with imatinib mesylate because of the residual tumor in the omentum. Formalin-fixed and paraffin-embedded specimens were used for histopathologic and immunohistochemical studies and for mutational analyses for the c-*kit* and *PDGFRA* genes. All GISTs were graded as high, intermediate, or low risk according to tumor size and to the MIB-1 grading system described elsewhere,[17] based on tumor differentiation, existence of tumor necrosis, and proliferating activity as estimated by Ki-67 (MIB-1) immunohistochemistry. Briefly, high-risk GISTs are >10 cm or are high grade (MIB-1–labeling index = 10% or tumor necrosis), intermediate-risk GISTs are >5 cm to 10 cm and are low grade (MIB-1–labeling index of <10% and no tumor necrosis), and low-risk GISTs are 5 cm and are low grade (Table 1).

Immunohistochemical Study

Immunohistochemical evaluation was performed by the avidin-biotin-peroxidase complex method in 3-μm-thick sections of formalin-fixed and paraffin-embedded specimens of GISTs and other mesenchymal tumors. We used polyclonal antibodies for KIT (DakoCytomation, Glostrup, Denmark: working dilution, 1:50; IBL, Fujioka, Japan: working dilution, 1:100), and a monoclonal antibody for CD34 (Becton Dickinson, Mountain View, CA: working dilution, 1:20). Cellular differentiation in GISTs was characterized by using the following antibodies: α-smooth muscle actin (DakoCytomation; monoclonal; working dilution, 1:500) and desmin (DakoCytomation; monoclonal; working dilution, 1:100) as markers for smooth muscle cells and by using the S100 protein (DakoCytomation; polyclonal, 1:1000) as a marker for Schwann cells. Ki-67 (MIB-1; MBL, Nogaoya, Japan: monoclonal, 1:100) was used to assess the proportion of proliferating cells, and the MIB-1–labeling index was estimated as reported elsewhere.[17] For antigen retrieval, formalin-fixed sections were pretreated in a microwave oven before incubation with the primary antibody.

We also performed toluidine blue staining for detection of mast cell infiltrations in GISTs. In the same KIT-stained sections of GISTs, we found many mast cell infiltrations between tumor cells. To accurately evaluate mast cell infiltrations in the tumors, toluidine blue staining was performed on all 3-μm-thick sections of formalin-fixed and paraffin-embedded specimens of GISTs in this study. For comparison, 24 cases of KIT-positive typical GISTs, all of which had c-*kit* gene mutations (23 in exon 11 mutations and 1 in exon 9) as shown by reverse-transcription polymerase chain reaction (PCR) and direct sequencing (data not shown), were also analyzed.

Sequencing Analyses of the C-*Kit* and *PDGFRA* Genes

Previously identified mutational hot spots in the c-*kit* and the *PDGFRA* gene in GISTs were analyzed. Genomic DNA was extracted from the 30 formalin-fixed and paraffin-embedded tumor tissues, by a standard proteinase K digestion method. Then the genomic DNA was amplified by PCR with the primers listed in Table 2 to amplify exons 9, 11, 13, and 17 of the c-*kit* gene and exons 12 and 18 of the *PDGFRA* gene. Each of the amplified fragments was purified from a polyacrylamide gel, and direct sequencing was performed with a Thermo Sequenase II Dye Terminator Cycle Sequencing Premix Kit (Amersham Biosciences, Piscataway, NJ) and with an ABI

TABLE 2. Sequences of Primers Used in This Study

Exon	Sequence
	c-kit
Exon 9F	5'-ATGCTCTGCTTCTGTACTGCC-3'
Exon 9R	5'-CAGAGCCTAAACATCCCCTTA-3'
Exon 11F	5'-CCAGAGTGCTCTAATGACTG-3'
Exon 11R	5'-ACCCAAAAAGGTGACATGGA-3'
Exon 13F	5'-CATCAGTTTGCCAGTTGTGC-3'
Exon 13R	5'-ACACGGCTTTACCTCCAAATG-3'
Exon 17F	5'-TGTATTCACAGAGACTTGGC-3'
Exon 17R	5'-GGATTTACATTATGAAAGTCACAGG-3'
	PDGFRA
Exon 12F	5'-TCCAGTCACTGTGCTGCTTC-3'
Exon 12R	5'-GCAAGGGAAAAGGGAGTCTT-3'
Exon 18F	5'-ACCATGGATCAGCCAGTCTT-3'
Exon 18R	5'-AAGTGTGGGAGGATGAGCCTG-3'

Abbreviation: PDGFRA, platelet-derived growth factor-α.

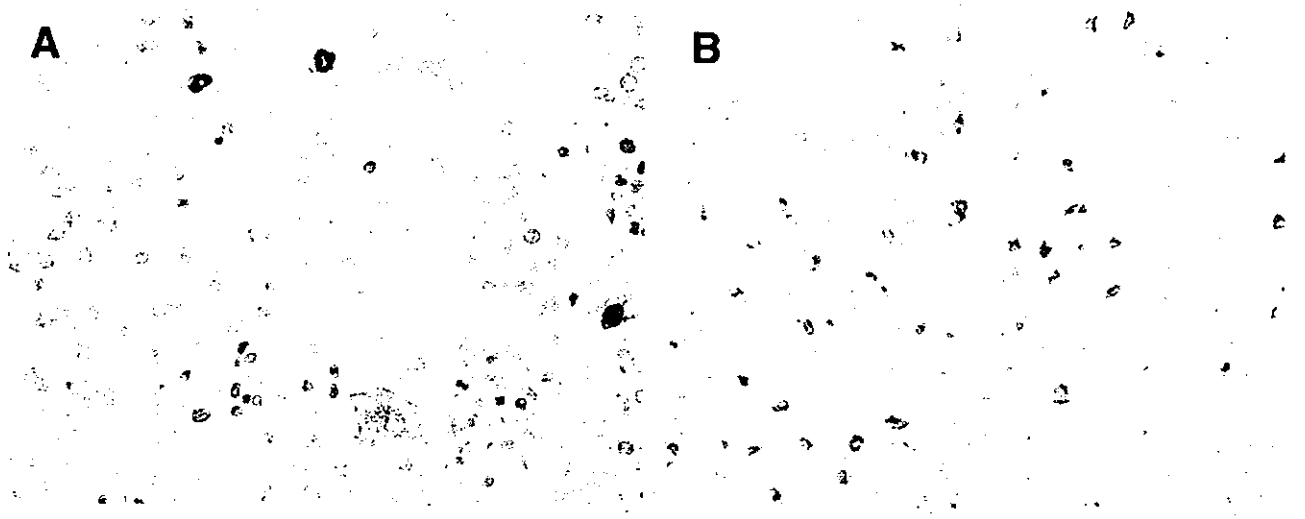

FIGURE 1. Immunostaining for KIT. All 27 gastrointestinal stromal tumors in this study were weak (A) or negative (B) for KIT. Strong immunoreactivity to KIT was observed in infiltrating mast cells in both cases.

PRISM 377 DNA Sequencer (Applied Biosystems, Foster City, CA), using the same primers as were used for PCR. All sequencing reactions were performed in both the forward and reverse directions.

Statistical Analyses

For the statistical analyses, we compared GISTs with and without myxoid epithelioid patterns (described in the results) and compared GISTs with or without the *PDGFRA* gene mutations. Gender, primary site, tumor grade, histological types, immunohistochemical phenotypes, and the existence of mast cell infiltrations were evaluated by Fisher's exact test or by χ^2 test. Age at surgery, maximum size of the tumors, and the MIB-1–labeling indexes were compared by Mann-Whitney U test.

RESULTS

Of the 30 GISTs examined in this study, 26 showed weak positive immunostaining for KIT according to our criteri, and the remaining cases (cases 20, 22, 25, and 26) were completely negative for KIT (Fig 1A and B). The clinicopathologic data resulting from the immunohistochemistry and mutational analyses of the c-*kit* and *PDGFRA* genes are presented in Table 3. The MIB-1–labeling index ranged from 1% to 21%. According to the criteria described above, 10 of the 30 tumors were classified as low risk, 6 as intermediate risk, and the remaining as high risk.

Histologically, all 30 GISTs showed epithelioid tumor cells in at least part of the tumor. Of these, we noticed that the tumor cells showed different morphology and arranged themselves in different patterns in each case with or without myxoid stroma. In cases 1, 2, 7, 11, 14, 19, 29, and 30, tumors consisted of both spindle and epithelioid tumor cells in varying ratios, and in the remaining cases, epithelioid cells occupied most parts of the tumor. In cases 1, 2, 3, 5, 7, 14, 17, 19, 27, and 29, the epithelial components of the tumor cells were mostly cohesive and arranged themselves in a sheetlike structure. Tumor cells in these cases showed clear or eosinophilic cytoplasm and centrally or peripherally placed nuclei (Fig. 2A).

On the other hand, in the remaining 17 cases of GISTs in this study, round or oval epithelioid tumor cells often showed a less cohesive pattern of growth and showed eosinophilic cytoplasm and peripherally placed nuclei with myxoid stroma. Multinucleated tumor cells were also seen in these tumors (Fig 2B), for which we used the term *myxoid epithelioid GISTs* in this study. Cases 6, 11, and 15, in which the myxoid epithelioid pattern was seen only in a part of the tumor, were also placed in this category.

Immunohistochemical Phenotypes

Of the 30 GISTs in the present study, 25 tumors were positive for CD34, and 13 tumors were weakly or focally positive for α-smooth muscle actin. Only 1 case was weakly positive for S100 protein, and 2 cases were weakly positive for desmin.

Mutations of the C-*kit* and *PDGFRA* Genes

Of the 30 GISTs examined here, 2 GISTs had c-*kit* gene mutations in exon 11 that were point mutations or in-frame deletions. *PDGFRA* gene mutations were found in 20 GISTs: 2 tumors had the same missense point mutation at codon 561 in exon 12, and the remaining tumors had in-frame deletions from codon 842 to 845 or had missense point mutations at codon 842 in exon 18. These are the same mutations of the *PDGFRA* gene in GISTs without the c-*kit* gene mutation, as previously reported. In the remaining 8 GISTs, mutations were not found in any exons of c-*kit* or *PDGFRA*.

TABLE 3. Clinicopathological Data Resulting From Immunohistochemistry and Mutational Analysis of the C-Kit and PDGFRA Gene in 27 Cases of KIT-Weak or KIT-negative GISTs

Case No.	Gender	Age	Primary Site	MIB-1 Size	MIB-1 LI (%)	MIB-1 Risk	Histology	Immunohistochemistry KIT	CD34	S100	SMA	Desmin	Mutations Gene	Mutations Site	Mast Cell Infiltration	Follow-Up Results (mo)
1	M	46	Small intestine	2.5	21	High	Spindle-cohesive epithelioid	Weak	+	+	–	–	—		—	DOD (22)
2	M	57	Esophagus	4.4	18	High	Spindle-cohesive epithelioid	Weak	+	–	–	–	c-kit	Exon 11 K558S, del V559	—	AW (16)
3	M	68	Stomach	7.5	<1	Int	Cohesive epithelioid	Weak	–	–	–	–	—		—	DOD (62)
4	M	60	Stomach	3.5	<1	Low	Myxoid epithelioid	Weak	+	–	–	–	PDGFRA	Exon 18 del DIMH842-845	+*	DOUD (364)
5	M	73	Stomach	3	8	Low	Cohesive epithelioid	Weak	–	–	+	–	—		—	AW (356)
6	M	46	Stomach	3	5	Low	Cohesive-myxoid epithelioid	Weak	+	–	–	–	—		—	AW (202)
7	F	71	Stomach	3.5	3	Low	Spindle-cohesive epithelioid	Weak	+	–	–	–	—		—	AW (190)
8	F	76	Stomach	2	9	Low	Myxoid epithelioid	Weak	+	–	+	–	PDGFRA	Exon 18 D842V	++†	AW (143)
9	M	43	Stomach	2.5	5	Low	Myxoid epithelioid	Weak	+	–	–	–	PDGFRA	Exon 18 D842V	—	AW (118)
10	M	44	Stomach	10	5	Int	Myxoid epithelioid	Weak	+	–	–	–	PDGFRA	Exon 18 del DIMH842-845	++	AW (101)
11	M	60	Stomach	12.5	3	High	Spindle-myxoid epithelioid	Weak	+	–	+	–	PDGFRA	Exon 18 del DIMH842-845, D846E	+	AW (96)
12	M	65	Stomach	3	3	Low	Myxoid epithelioid	Weak	+	–	–	–	—		+	AW (75)
13	M	50	Stomach	21	10	High	Myxoid epithelioid	Weak	+	–	+	+	PDGFRA	Exon 18 del DIMH842-845	+	AW (43)
14	M	62	Stomach	2.5	15	High	Spindle-cohesive epithelioid	Weak	+	–	–	+	c-kit	Exon 11 del MYEV552-555	—	AW (6)
15	M	46	Stomach	1.2	11	High	Cohesive-myxoid epithelioid	Weak	+	–	+	–	PDGFRA	Exon 18 D842V	—	AW (6)
16	F	73	Omentum	4	3	Low	Myxoid epithelioid	Weak	+	–	+	–	PDGFRA	Exon 18 D842V	++	AW (4)
17	M	52	Omentum	>20	4	High	Cohesive epithelioid	Weak	–	–	–	–	PDGFRA	Exon 18 del DIMH842-845	+	AW (13)
18	F	80	Stomach	3.7	3	Low	Myxoid epithelioid	Weak	+	–	–	–	PDGFRA	Exon 12 V561D	++	AW (3)
19	M	51	Stomach	2.5	2	Low	Spindle-cohesive epithelioid	Weak	+	–	+	–	—		—	DOUD (171)
20	M	65	Stomach	8	1	Int	Myxoid epithelioid	—	–	–	–	–	PDGFRA	Exon 12 V561D	++	ND
21	M	49	Stomach	8	14	High	Myxoid epithelioid	Weak	+	–	+	–	PDGFRA	Exon 18 del DIMH842-845	+	AW (12)
22	M	66	Stomach	1.2	49	Low	Myxoid epithelioid	—	–	–	–	–	PDGFRA	Exon 18 D842V	++	ND
23	M	54	Stomach	1.1	3	Low	Myxoid epithelioid	Weak	+	–	–	–	PDGFRA	Exon 18 D842V	++	AW (12)
24	M	74	Stomach	6	4.5	Int	Myxoid epithelioid	Weak	+	–	+	–	PDGFRA	Exon 18 D842V	+	AW (24)
25	F	36	Stomach	2.2	7.5	Low	Myxoid epithelioid	—	+	–	–	–	PDGFRA	Exon 18 del DIMH842-845	+	AW (9)
26	M	57	Stomach	6	5	Int	Myxoid epithelioid	—	+	–	+	–	PDGFRA	Exon 18 del DIMH842-845	+	AW (5)
27	F	64	Stomach	4	<1	Low	Cohesive epithelioid	Weak	+	–	–	–	—	—	AW (40)	
28	M	69	Stomach	6.5	2	Int	Myxoid epithelioid	Weak	+	–	+	–	PDGFRA	Exon 18 D842V	++	AW (1)
29	M	50	Stomach	4	5	Low	Spindle-cohesive epithelioid	Weak	+	–	+	–	PDGFRA	Exon 18 D842V	—	AW (3)
30	M	76	Stomach	2.3	9	Low	Spindle-myxoid epithelioid	Weak	+	–	+	–	PDGFRA	Exon 18 D842V	++	AW (1)

Abbreviations: PDGFRA, platelet-derived growth factor-α; GIST, gastrointestinal stromal tumor; LI, labeling index; SMA, smooth muscle actin; DOD, died of disease; del, deletion; AW, alive and well; int, intermediate; DOUD, died of unrelated disease; ND, no data available.

*For most cell infiltration instances.

†Numerous most cell infiltration instances present within a tumor nodule.

GISTs With or Without Mast Cell Infiltration

Mast cells were clearly detected by their characteristic metachromatic staining with toluidine blue. Infiltration of mast cells within the tumor nodules was observed in 18 of the 30 GISTs (60%; Fig 3A), although the number of infiltrating mast cells was varied in each case (Table 3). In contrast, no mast cell infiltration of 24 KIT-positive GISTs with c-*kit* gene mutations was observed (Fig 3B).

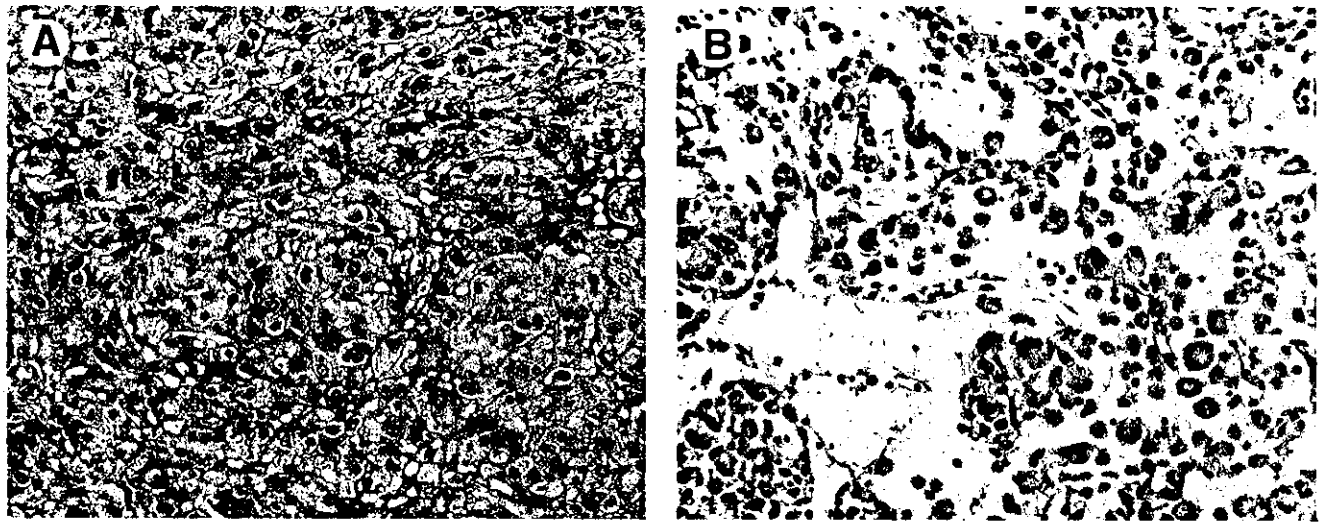

FIGURE 2. Epithelioid components of gastrointestinal stromal tumors in this study showed different histology. (A) Tumor cells in this case showed clear cytoplasm and centrally or peripherally placed nuclei and were mostly cohesive and arranged themselves in a sheetlike structure. (B) Tumor cells in other cases showed less cohesive patterns of growth and showed eosinophilic cytoplasm and peripherally placed nuclei with myxoid stroma. Multinucleated tumor cells were also seen in these tumors. Hematoxylin and eosin staining.

KIT-Weak or KIT-Negative GISTs With or Without Myxoid Epithelioid Patterns

The clinicopathologic data including other immunohistochemical data, the existence of mast cell infiltrations in the tumor nodules, and mutations of the c-*kit* or *PDGFRA* gene were compared between the 27 GISTs with or without myxoid epithelioid patterns (Table 4). The gender, age at initial operation, primary sites and sizes of tumors, MIB-1–labeling index and tumor risk, and immunohistochemical phenotypes were not different between the 2 groups. Mast cell infiltrations within the tumor nodules were preferentially observed in the GISTs with a myxoid epithelioid pattern ($P < 0.0001$). Only 1 weakly KIT-positive large GIST (case 19) without a myxoid epithelioid pattern was accompanied by mast cell infiltration. The presence or site of mutations in the *c-kit* or *PDGFRA* genes was significantly different between GISTs with and without a myxoid epithelioid pattern ($P < 0.0001$). Mutations in the *PDGFRA* gene were preferentially found in the GISTs with a myxoid epithelioid pattern (18 of 20, 90%), whereas only 2 of the 10 GISTs without a myxoid epithelioid pattern had a *PDGFRA* gene mutation (case 17). Two cases in GISTs without a myxoid epithelioid pattern (cases 2, 14) had a point mutation or an in-frame deletion in exon 11 of the c-*kit* gene.

Prognosis of the patients with KIT-weak or KIT-negative GISTs was as follows. Twenty-eight patients were followed for 1 to 364 months (mean, 82 months; median, 42 months). Four of the 28 patients died dur-

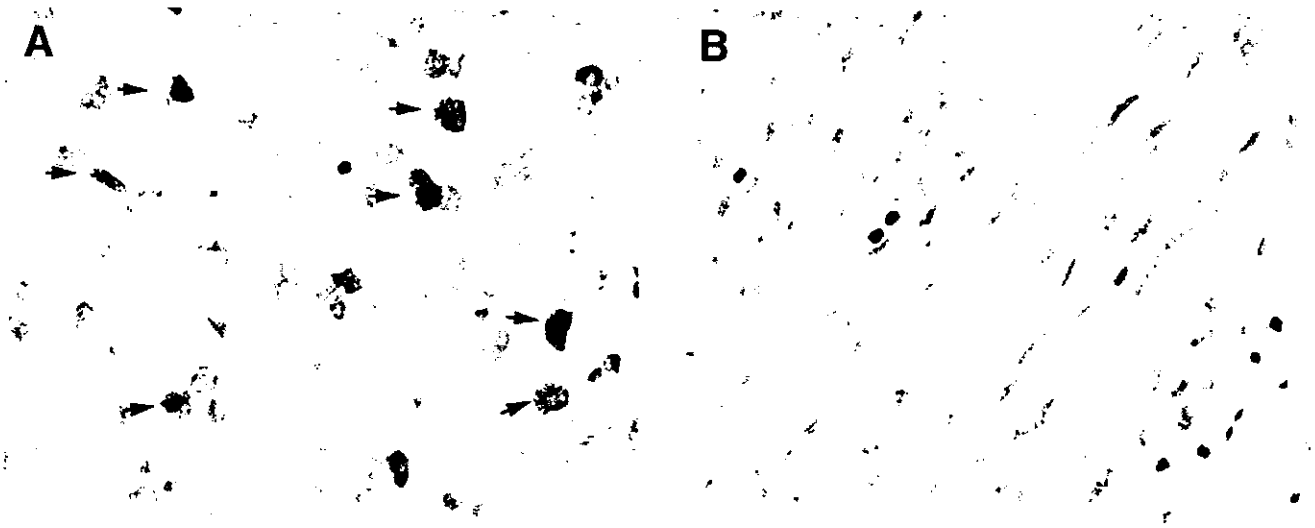

FIGURE 3. Mast cell infiltrations were frequently observed in KIT-weak or KIT-negative gastrointestinal stromal tumors (GISTs; arrow; A) but not in KIT-positive GISTs with *c-kit* gene mutations (B). Toluidine blue staining.

TABLE 4. Comparison of Clinicopathological and Immunohistochemical Data and Mutational Analysis of the C-Kit and PDGFRA Gene Between Myxoid Epithelioid GISTs and Others

Variable	KIT-Weak or KIT-Negative GISTs		*P* Value
	Myxoid Epithelioid GISTs (n = 20)	Others (n = 10)	
Gender (male:female)	16:4	9:1	NS
Age (yr)	36-80 (average, 59.5)	46-73 (average, 59.4)	NS
Site (eso/st/SI/ome)	0/20/0/1	1/7/1/1	NS
Size	5.4 ± 4.8	5.4 ± 5.3	NS
MIB-1 LI	5.4 ± 3.5	7.8 ± 7.5	NS
Grade (high/int/low)	4/5/11	4/1/5	NS
Immunohistory			
CD34	18/20	7/10	NS
SMA	10/20	3/10	NS
S100	0/20	1/10	NS
Desmin	1/20	1/10	NS
Mast cell infiltration	17/20	1/10	0.0001
Mutation (c-kit/PDGFRA/negative)	0/18/2	2/2/6	0.0001

Abbreviations: PDGFRA, platelet-derived growth factor-α; GIST, gastrointestinal stromal tumor; NS, statically not significant; eso, esophagus; St, stomach; SI, small intestine; LI, labeling index; SMA, smooth muscle actin.

ing the follow-up period, of which 2 deaths were caused by the primary disease (cases 1 and 3, each 22 and 62 months after initial operations) and the remaining deaths were caused by unrelated disease (cases 4 and 19). GISTs in cases 1 and 3 had no myxoid epithelioid component in the tumor cells or mutations in the c-*kit* and *PDGFRA* genes. None of the patients with myxoid epithelioid GISTs or GISTs with *PDGFRA* gene mutations died of disease during follow-up periods, although 1 patient had a residual tumor at the primary site (case 17).

DISCUSSION

In recent years, the diagnosis and treatment of GISTs has advanced and changed dramatically. Most GISTs consist of spindle cells showing fascicular patterns and are immunohistochemically positive for KIT.[8-12] Moreover, gain-of-function mutations in the c-*kit* gene are found in these KIT-positive GISTs.[8,13] Now, GISTs are defined as KIT-positive mesenchymal tumors in the gastrointestinal tract and are distinguished from other mesenchymal tumors. Recently, molecular targeting treatments with imatinib mesylate (STI571), which is a KIT tyrosine kinase inhibitor, have been given to patients with KIT-positive GISTs, with reports of significant effectiveness for metastatic and unresectable GISTs.[18,19]

However, it is known that some GISTs are immunohistochemically weak or negative for KIT. In such cases, the accurate diagnosis of GISTs might be difficult for pathologists, although the pathologic diagnosis is indispensable for correctly prescribing imatinib mesylate.

More recently, *PDGFRA* gene mutations have been reported in some GISTs without c-*kit* gene mutations that also can be effectively treated with imatinib mesylate.[14,15,20] However, the clinicopathologic and histological characteristics of GISTs with *PDGFRA* gene mutations have not been fully analyzed previously.

Overall, 30 of 303 GISTs (9.9%) were weak or negative for KIT and were analyzed in this study. All 30 GISTs consisted of epithelioid tumor cells exclusively or focally, although epithelioid GISTs are seen in about 20%-30% of all GISTs in general.[4,5,21] Of 273 KIT-positive GISTs in our cases, 226 (83%) GISTs were shown to be the spindle cell type, 38 (14%) were shown to be the mixed (combination of spindle and epithelioid cell) type, and 9 (3%) were shown to be the epithelioid cell type (data not shown). Histologically, we noticed different patterns within the epithelioid tumor cells in KIT-weak or KIT-negative GISTs. In some epithelioid GISTs, tumor cells arranged themselves in tightly cohesive patterns. In others, tumor cells loosely arranged themselves and were accompanied by myxoid stroma. We called the latter type of GISTs *myxoid epithelioid GISTs* in our study. Interestingly, subsequent mutational analyses showed a close relationship between these histological patterns and the type of mutations. Myxoid epithelioid GISTs closely correlated with *PDGFRA* gene mutations in both exons 12 and 18.

The *PDGFRA* gene mutations were found in 20 of the 30 KIT-weak or KIT-negative GISTs (66.6%). This rate is higher than that reported by Heinrich et al,[14] in whose study *PDGFRA* gene mutations were found in about 35% of GISTs without c-*kit* gene mutations. The rate became much higher when the cases were limited to the 20 myxoid epithelioid GISTs, of which 18 (90%) had *PDGFRA* gene mutations.

On the other hand, of 273 KIT-positive GISTs, 11 tumors were also accompanied by myxoid stroma, and 3 of those were of the epithelioid cell type resembling histology of myxoid epithelioid GISTs in this study. However, those 3 cases had mutations in the c-*kit* gene exon 11 but not in the *PDGFRA* gene (data not shown). Thus, the histology of myxoid epithelioid pattern in

KIT-weak or KIT-negative GISTs is considerably specific to GISTs with *PDGFRA* gene mutations. In only 2 GISTs with *PDGFRA* gene mutations (cases 17 and 29) were the GISTs not myxoid epithelioid. The tumor in case 17 was large and classified as high risk. Tumor progression may have influenced the morphology and growth pattern of the tumor cells in this case, although the tumor in case 29 was relatively small and was classified as low risk. In cases 6 and 12, *PDGFRA* gene mutations were not identified despite having a myxoid epithelioid pattern. However, the c-*kit* gene mutations were also not present in these cases. Mutations in other exons of the *PDFFRA* gene that we did not examine in this study might be present in these 2 tumors. Furthermore, we also found close relationships between myxoid epithelioid GISTs or GISTs with *PDGFRA* gene mutations and mast cell infiltration. In general, we frequently found mast cell infiltrations in various degrees in leiomyomas and leiomyosarcomas in the gastrointestinal tract and uterus.[22,23] Previous reports indicated that the numbers of mast cells within and around tumor nodules were thought to be a useful prognostic factor for soft tissue sarcomas.[23-25] In contrast, infiltrations of mast cells were observed in none of the KIT-positive GISTs with c-*kit* gene mutations in this study. We have used this histological difference for distinguishing between GISTs and other soft tissue tumors for some time. However, mast cell infiltration was observed in 18 of 30 GISTs (60%) in this study. Of these, 17 tumors were myxoid epithelioid GISTs (17 of 20, 85%). There is a close correlation between mast cell infiltrations and myxoid epithelioid patterns or *PDGFRA* gene mutations in GISTs ($P < 0.0001$). Very recently, Debiec-Rychter et al[26] also reported *PDGFRA* gene mutations in 3 (43%) of 7 KIT-negative GISTs, whereas their remaining tumors had no mutation in either c-*kit* or *PDGFRA* genes. In their reports, mast cell infiltrations were also seen within tumor nodule. Incidentally, mast cell infiltrations were not observed in 2 of 3 KIT-positive tumors resembling myxoid epithelioid GISTs in this study (data not shown).

At present, we have no evidence that explains the presence or absence of mast cell infiltrations among different types of GISTs. Stem cell factor (SCF), a natural ligand of the KIT receptor, is thought to be produced by smooth muscle cells and neurons in the gastrointestinal tract.[27,28] Mast cell infiltrations within leiomyomas and leiomyosarcomas are probably caused by SCF production by tumor cells that are of smooth muscle cell origin. On the other hand, SCF expression by tumor cells of GISTs has not been reported until now. However, we confirmed mRNA expression of both membrane-bound and soluble isoforms of SCF in all the KIT-positive GISTs by reverse-transcription PCR (data not shown). Rapid internalization of SCF by the SCF–KIT juxtacrine loop between tightly cohesive tumor cells may prevent mast cell infiltration in KIT-positive GISTs but not in myxoid epithelioid GISTs, which are less cohesive and weak or negative for KIT. Further studies about SCF expression in KIT-positive and KIT-weak or KIT-negative GISTs will be needed to explain the mechanism of mast cell infiltration in myxoid epithelioid GISTs.

GISTs are thought to originate from the ICCs because of the phenotypic similarity of specific molecules such as KIT, CD34, Smemb, and nestin.[8-12] However, in the human small intestine, a slow wave is also detected at the deep muscular plexus level, where KIT-positive ICCs are not present.[29] We previously observed KIT-negative, CD34-positive, ICC-like cells adjacent to KIT-positive ICCs in the stomach and small intestine.[11] The existence of KIT-negative fibroblast-like cells adjacent to KIT-positive ICCs has been reported.[30,31] GISTs with *PDGFRA* gene mutations may originate from such KIT-negative ICCs or other unknown mesenchymal cells, and that may reflect differences of histology and KIT expression. Further search and classification of ICCs and related mesenchymal cells and analysis of *PDGFRA* expression in such mesenchymal cells will be needed to confirm this hypothesis.

Although none of the patients with GISTs containing *PDGFRA* mutations died of disease, follow-up periods in this study are too short to conclude benign behavior of GISTs with *PDGFRA* mutations. Five of the 20 GISTs with the *PDGFRA* gene mutations were classified as high risk, and 1 of those (case 17) was treated with imatinib mesylate because of the residual tumor in the omentum. At present, the patient remains in partial remission. In this case, the mutation was deletion DIMH842-845 in exon 18 of the *PDGFRA* gene, and GISTs with this type of mutation have been reported to be sensitive to treatment with imatinib mesylate.[20] Mutational analysis and molecular subclassification of GISTs are now more important since the introduction of imatinib mesylate, because clinical responses to the drug and prognosis of patients are different in GISTs with different mutations.[20] However, the time and costs involved in analyzing all mutational hot spots in the c-*kit* and *PDGFRA* genes in GISTs present a problem for routine pathologic diagnosis. The results of this study suggest that it is best to analyze mutations in the *PDGFRA* gene first in myxoid epithelioid GISTs with mast cell infiltrations.

In conclusion, we analyzed 30 GISTs that were weak or negative for KIT in this study. We discovered a close correlation between a specific histological type of GISTs, myxoid epithelioid GISTs, and *PDGFRA* gene mutations. Myxoid epithelioid GISTs were accompanied by mast cell infiltrations that were not found in other types of GISTs. These histological characteristics may be useful for subsequent mutational analysis and molecular subclassification of GISTs.

REFERENCES

1. Mazur MT, Clark HB: Gastric stromal tumors: Reappraisal of histogenesis. Am J Surg Pathol 7:507-519, 1983

2. Ueyama T, Guo KJ, Hashimoto H, et al: A clinicopathologic and immunohistochemical study of gastrointestinal stromal tumors. Cancer 69:947-955, 1992

3. Franquemont DW, Frierson HF Jr: Muscle differentiation and

clinicopathological features of gastrointestinal stromal tumors. Am J Surg Pathol 16:947-954, 1992

4. Fletcher CD, Berman JJ, Corless C, et al: Diagnosis of gastrointestinal stromal tumors: A consensus approach. Hum Pathol 33: 459-465, 2002

5. Miettinen M, Lasota J: Gastrointestinal stromal tumors—definition, clinical, histological, immunohistochemical, and molecular genetic features and differential diagnosis. Virchows Arch 438:1-12, 2001

6. Ward SM, Burns AJ, Torihashi S, et al: Mutation of the proto-oncogene c-kit blocks development of interstitial cells and electrical rhythmicity in murine intestine. J Physiol 480:91-97, 1994

7. Burns AJ, Lomax AE, Torihashi S, et al: Interstitial cells of Cajal mediate inhibitory neurotransmission in the stomach. Proc Natl Acad Sci U S A 93:12008-12013, 1996

8. Hirota S, Isozaki K, Yasuhiro M, et al: Gain-of-function mutations of c-kit in human gastrointestinal stromal tumors. Science 279: 577-580, 1998

9. Sarlomo-Rikala M, Kovatich AJ, et al: CD117: A sensitive marker for gastrointestinal stromal tumors that is more specific than CD34. Mod Pathol 11:728-734, 1998

10. Kindblom LG, Remotti HE, Aldenborg F, et al: Gastrointestinal pacemaker cell tumor (GIPACT): Gastrointestinal stromal tumors show phenotypic characteristics of the interstitial cells of Cajal. Am J Pathol 152:1259-1269, 1998

11. Sakurai S, Fukasawa T, Chong JM, et al: Embryonic form of smooth muscle myosin heavy chain (SMemb/MHC-B) in gastrointestinal stromal tumor and interstitial cells of Cajal. Am J Pathol 154: 23-28, 1999

12. Tsujimura T, Makiishi-Shimobayashi C, Lundkvist J, et al: Expression of the intermediate filament nestin in gastrointestinal stromal tumors and interstitial cells of Cajal. Am J Pathol 158:817-823, 2001

13. Rubin BP, Singer S, Tsao C, et al: KIT activation is a ubiquitous feature of gastrointestinal stromal tumors. Cancer Res 61:8118-8121, 2001

14. Heinrich MC, Corless CL, Duensing A, et al: PDGFRA activating mutations in gastrointestinal stromal tumors. Science 299:708-710, 2003

15. Hirota S, Ohashi A, Nishida T, et al: Gain-of-function mutations of platelet-derived growth factor receptor alpha gene in gastrointestinal stromal tumors. Gastroenterology 125:660-667, 2003

16. Wardelmann E, Neidt I, Bierhoff E, et al: c-kit mutations in gastrointestinal stromal tumors occur preferentially in the spindle rather than in the epithelioid cell variant. Mod Pathol 15:125-136, 2002

17. Hasegawa T, Matsuno Y, Shimoda T, et al: Gastrointestinal stromal tumor: Consistent CD117 immunostaining for diagnosis, and prognostic classification based on tumor size and MIB-1 grade. Hum Pathol 33:669-676, 2002

18. van Oosterom AT, Judson I, Verweij J, et al: Safety and efficacy of imatinib (STI571) in metastatic gastrointestinal stromal tumors: A phase I study. Lancet 358:1421-1423, 2001

19. Demetri GD, von Mehren M, Blanke CD, et al: Efficacy and safety of imatinib mesylate in advanced gastrointestinal stromal tumors. N Engl J Med 347:472-480, 2002

20. Heinrich MC, Corless CL, Demetri GD, et al: Kinase mutations and imatinib response in patients with metastatic gastrointestinal stromal tumor. J Clin Oncol 21:4342-4349, 2003

21. Miettinen M, Sarlomo-Rikala M, Lasota J: Gastrointestinal stromal tumors: Recent advances in understanding of their biology. Hum Pathol 30:1213-1220, 1999

22. Maluf HM, Gersell DJ: Uterine leiomyomas with high content of mast cells. Arch Pathol Lab Med 118:712-714, 1994

23. Yavuz E, Gulluoglu MG, Akbas N, et al: The values of intratumoral mast cell count and Ki-67 immunoreactivity index in differential diagnosis of uterine smooth muscle neoplasms. Pathol Int 51:938-941, 2001

24. Ueda T, Aozasa K, Tsujimoto M, et al: Prognostic significance of mast cells in soft tissue sarcoma. Cancer 62:2416-2419, 1988

25. Tomita Y, Aozasa K, Myoui A, et al: Histologic grading in soft-tissue sarcomas. An analysis of 194 cases including AgNOR count and mast-cell count. Int J Cancer 54:194-199, 1993

26. Debiec-Rychter M, Wasag B, Stul M, et al: Gastrointestinal stromal tumors (GISTs) negative for KIT (CD 117 antigen) immunoreactivity. J Pathol 202:430-438, 2004

27. Ward SM, Ordog T, Bayguinov JR, et al: Development of interstitial cells of Cajal and pacemaking in mice lacking enteric nerves. Gastroenterology 117:584-594, 1999

28. Wu JJ, Rothman TP, Gershon MD: Development of the interstitial cell of Cajal: Origin, Kit dependence and neuronal and nonneuronal sources of Kit ligand. J Neurosci Res 59:384-401, 2000

29. Torihashi S, Horisawa M, Watanabe Y: c-kit immunoreactive interstitial cells in the human gastrointestinal tract. J Auton Nerv Syst 75:38-50, 1999

30. Vanderwinden JM, Rumessen JJ, de Kerchove d'Exaerde A Jr, et al: Kit-negative fibroblast-like cells expressing SK3, a Ca2+-activated K+ channel, in the gut musculature in health and disease. Cell Tissue Res 310:349-358, 2002

31. Fujita A, Takeuchi T, Jun H, Hata F: Localization of Ca2+-activated K+ channel, SK3, in fibroblast-like cells forming gap junctions with smooth muscle cells in the mouse small intestine. J Pharmacol Sci 92:35-42, 2003

Pathology International 2004; **54**: 675–681

Original Article

Immunohistochemical study of Skp2 and Jab1, two key molecules in the degradation of P27, in lung adenocarcinoma

Akiteru Goto,[1] Toshiro Niki,[1] Sachiko Moriyama,[2] Nobuaki Funata,[2] Hirokazu Moriyama,[3] Yoshihiro Nishimura,[3] Rika Tsuchida,[4] Jun-ya Kato[5] and Masashi Fukayama[1]

[1]Department of Human Pathology, Graduate School of Medicine, The University of Tokyo, Departments of [2]Pathology and [3]Surgery, Tokyo Metropolitan Komagome Hospital, [4]Department of Pediatrics, Tokyo Medical and Dental University, Tokyo and [5]Graduate School of Biological Sciences, Nara Institute of Science and Technology, Nara, Japan

To clarify the association of the P27 degradation pathway proteins, Skp2 and Jab1, with the development and progression of lung adenocarcinoma (AD), we immunohistochemically investigated Skp2 and Jab1 expression together with P27- and Ki-67-labeling in 110 lung AD and 11 atypical adenomatous hyperplasia (AAH) and analyzed the relationship between the expression of these proteins and the clinicopathological factors. High Skp2 or Jab1 expression was frequent in lung AD (52/110, 47%, and 59/110, 54%, respectively), and high expression of Jab1 was also frequent in AAH (4/11, 36%), while it was not observed in normal bronchiolar epithelium. The P27 labeling index (LI) was reciprocally correlated with high Skp2 and Jab1 expression, and a higher Ki-67 LI was significantly correlated with high Skp2 and Jab1 expression. However, low P27 expression did not correlate with a higher Ki-67 LI. High Skp2 lung AD showed significant correlation with blood and lymphatic vessel invasion, which low P27 expression did not correlate with. Furthermore, high Skp2 expression in lung AD was significantly correlated with a poor outcome for patients. Thus, Skp2 and Jab1 regulate P27 degradation, and might contribute to the development and progression of lung AD through P27-mediated and –unmediated mechanisms.

Key words: atypical adenomatous hyperplasia, Jab1, Ki-67, lung adenocarcinoma, P27 (kip1), prognosis, Skp2

Genetic and epigenetic alterations of cell cycle regulators are key abnormalities in the development and progression of carcinoma, including lung adenocarcinoma (AD).[1–6] P27 (kip1) is an inhibitor of G1 kinases and a negative regulator of cell proliferation,[7] and its loss of function is almost certainly involved in the development of lung AD.[5,6] However, the mechanisms underlying its loss of function in lung AD still remain to be understood. P27 alteration in lung AD is likely to be induced post-translationally, since *P27* mRNA expression is reportedly retained in lung AD[6] and genetic alterations of *P27* have rarely been observed in various cancers.[8]

There are two key molecules involved in post-translational regulation of P27. One is S-phase kinase-interacting protein 2 (Skp2), which has been shown to be required for ubiquitin-mediated degradation of P27.[9,10] The other is Jun activation domain-binding protein-1 (Jab1), a nuclear export protein, which targets P27 for transportation from the nucleus to cytoplasm, and Jab1 promotes the subsequent degradation of P27.[11,12] Overexpression of Skp2 or Jab1 has been observed with reciprocal correlation to P27 expression in various malignancies, including small cell lung carcinoma, oral squamous cell carcinoma, gastric carcinoma, diffuse-large B cell lymphoma, embryonal rhabdomyosarcoma and breast carcinoma.[13–18] Among these malignancies, the prognostic significance of Skp2 overexpression is reported in gastric cancer and diffuse-large B cell lymphoma.[15,16] Despite the demonstrated importance of Skp2 and Jab1 in tumor biology, to the best of our knowledge the significance of Skp2 or Jab1 in tumorigenesis of lung AD has not been addressed, and the prognostic significance of these proteins in lung AD has not been clarified. Furthermore, the observation of both Skp2 and Jab1 on the same clinical specimens has not been reported in any tumor. Thus, in the present study, we concurrently evaluated the abnormal expression of Skp2 and Jab1 by immunohistochemistry with comparative analysis of P27 expression and proliferative activity in the surgically resected lung AD and atypical adenomatous hyperplasias (AAH), a putative precancerous lesion of lung AD.[19] The aim of the present study is to clarify the significance of the P27 degradation pathway proteins, Skp2 and Jab1, in the development and progression of lung AD.

Correspondence: Akiteru Goto, MD, PhD, Department of Human Pathology, Graduate School of Medicine, University of Tokyo, 7-3-1, Hongo, Bunkyo-ku, Tokyo 113-0033, Japan.
Email: akiteru@m.u-tokyo.ac.jp

Received 25 December 2003. Accepted for publication 30 April 2004.

MATERIALS AND METHODS

Patients and tissues

We examined a series of 121 peripheral neoplastic lesions of the lung. They consisted of 11 lesions of atypical adenomatous hyperplasia (AAH) and 110 lesions of small lung adenocarcinomas (AD) (maximum diameter, 3 cm or less). The specimens were obtained from 121 patients who underwent pneumonectomy or lobectomy without preoperative chemotherapy or radiotherapy. All samples were collected from the surgical pathology files at Tokyo Metropolitan Komagome Hospital and University of Tokyo Hospital, Tokyo, Japan, between 1977 and 2000. The patients were comprised of 72 males and 49 females. The age of the patients ranged from 32 to 89 years, with an average of 61.1 years. For lung AD, the observation periods ranged from 1 month to 163 months, with a median follow-up period of 66.2 months. The patients with lung AD were staged according to the tumor-node-metastasis system adopted by the American Joint Committee on Cancer and the International Union Against Cancer.[20] The cases consisted of 53 Stage I (31 Stage IA and 22 Stage IB), six Stage II (two Stage IIA and four Stage IIB), 50 Stage III (37 Stage IIIA and 13 Stage IIIB) and one Stage IV. Histological differentiation of tumors was graded according to the criteria described in the Japanese General Rule for Clinical and Pathological Record of Lung Cancer.[21] Lung AD was also histologically evaluated for lymph node metastasis (n), pleural infiltration (p), pleural dissemination (d), intrapulmonary metastasis (pm), blood vessel invasion (v) and lymphatic vessel invasion (ly). For the evaluation of pleural infiltration (p) and blood vessel invasion (v), elastica van Gieson stain of the sections was routinely used to identify the elastic fibers of pleura and blood vessels.

Immunohistochemistry

All resected specimens were fixed in 10% buffered formalin and embedded in paraffin. Sections (4 μm thick) were cut and deparaffinised through graded alcohol and xylene. After antigen retrieval with autoclave treatment in 10 mmol/L citrate buffer, pH 6.0, endogeneous peroxidase was blocked with 3% hydrogen peroxide in methanol for 20 min. The sections were washed three times with cold 0.01 mol/L phosphate-buffered saline (PBS). After blocking with 10% normal rabbit serum, the sections were incubated for 16 h at 4°C with rabbit polyclonal antibody against human Skp2 protein (diluted at 1:75; Santa Cruz Biotechnology, Inc., Santa Cruz, CA, USA), rabbit polyclonal antibody against Jab1 protein (1:300),[11,17] mouse monoclonal antibody against human P27 (1:100; BD Transduction Laboratories, Lexington, KY, USA) and mouse monoclonal antibody against human Ki-67 (Mib1, 1:100; DakoCytomation, Copenhagen, Denmark). The sections were incubated with biotinated goat antirabbit immunoglobulin G (IgG) or rabbit antimouse IgG, and reacted with the streptavidin-biotin peroxidase reagent (LSAB2 Kit, DakoCytomation). Finally, the reaction was visualized with a chromogen, 3-3′-diaminobenzidine (30 mg in 100 mL of 0.05 mol/L Tris Buffer pH 7.6 with 17 μL of hydrogen peroxidase). Sections were then counterstained with hematoxylin, dehydrated and mounted. Sections of human tonsil were used as positive controls for Skp2, Jab1 and Ki-67 immunohistochemistry. For P27, normal bronchiolar epithelial cells, distant from the tumor by at least 2 cm, were used as an internal positive control. Negative controls were obtained by omitting primary antibodies.

Assessment of Skp2, Jab1, P27 and Ki-67 immunoreactivities

The labeling index (LI) for each protein was determined in each tumorous lesion and in normal bronchiolar regions of the background lungs without any pathological process (10 cases of lung AD). The LI was determined by calculating the percentage of positively immunostained cells in 2000 cells. In some smaller AAH lesions, all the cells in the entire area of the lesion were counted (250–600 cells per lesion). Immunohistochemical results were subdivided into two categories, high (or overexpression) and low, according to the subjective judgment that the LI had a bipolar distribution with an appropriate cut-off number for each molecule, such as 10% of tumor cells for Skp2, 30% for Jab1, 20% for P27 and 30% for Ki-67. Faint staining of cells was not considered to be positive.

Statistical analysis

Calculations were performed using StatviewJ-4.02 (Abacus Concepts Inc., USA.) software. Differences in mean values between the groups were analyzed by the Student's *t*-test. Interaction of the factors was examined by variance analysis. Differences in frequency were analyzed by the chi-squared test. Kaplan–Meier plots and the log-rank test were used for survival analysis. A result was considered significant if the *P*-value was <0.05.

RESULTS

The results of immunohistochemistry for Skp2, Jab1, P27 and Ki-67 are summarized in Table 1.

Table 1 Skp2 and Jab1 overexpressions in lung bronchiolar epithelium, AAH and adenocarcinoma

	Normal bronchiolar epithelium	AAH	Adenocarcinoma
Skp2 overexpression (%)	0/15 (0)	2/11 (22.2)	52/110 (47.3)
		*	*
	*		
Jab1 overexpression (%)	0/15 (0)	4/11 (36.4)	59/110 (53.6)
		*	
	*		*

AAH, atypical adenomatous hyperplasia. *$P < 0.05$.

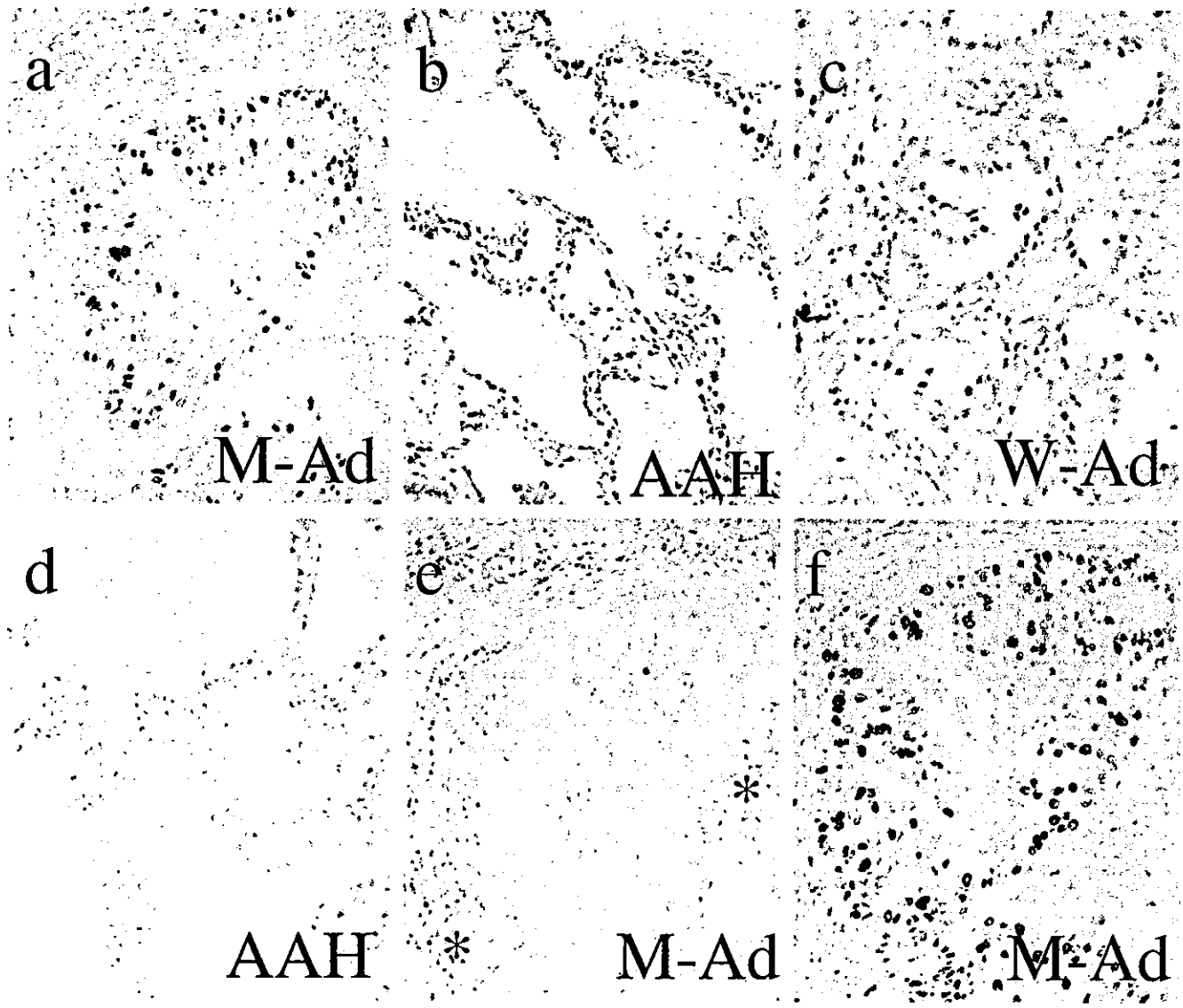

Figure 1 Immunohistochemical staining of (**a**,**b**) Skp2, (**c**,**d**) Jab1, (**e**) P27 and (**f**) Ki-67 in lung adenocarcinoma and atypical adenomatous hyperplasia (AAH). (**a**) Moderately differentiated adenocarcinoma and (**b**) AAH showing nuclear staining of Skp2 (>10% nuclei positive). (**c**) Well-differentiated adenocarcinoma and (**d**) AAH showing nuclear staining of Jab1 (>30% nuclei positive). (**e**) Moderately differentiated adenocarcinoma, in which most cells showed negative staining of P27, except for interstitial lymphocytes (*). (**f**) Moderately differentiated adenocarcinoma showing nuclear staining of Ki-67 with a labeling index of more than 30%. (**a**), (**e**) and (**f**) are photographs of the serial sections of the adenocarcinoma case. AAH, atypical adenomatous hyperplasia; M-Ad, moderately differentiated adenocarcinoma; W-Ad, well-differentiated adenocarcinoma.

Skp2 and Jab1 immunoreactivies in the lung and lung tumor

Both Skp2 and Jab1 immunoreactivities were observed in neoplastic epithelial cells of the lung. Skp2 immunoreactivity was almost exclusively confined to the nucleus of the neoplastic cells and Jab1 immunoreactivity was also observed in the nuclei of the cells, although faint staining was sometimes present in the cytoplasm (Fig. 1a–d). Skp2 overexpression was more frequently observed in AD than in AAH or in BE with statistical significance. Jab1 overexpression was more frequently observed in AD or AAH than in BE (Table 1).

Relationship of high Skp2 and Jab1 expressions with the P27 and Ki-67 labeling indexes

To evaluate the relationship of high Skp2 and Jab1 expressions with a P27 or proliferative component, P27 and Ki-67 labeling indexes were obtained. P27 immunoreactivity was consistently found in the nuclei of lymphocytes or normal bronchial epithelial cells entrapped in the neoplastic lesions, which served as internal positive controls (Fig. 1e). The labeling index (LI) of P27 was higher in BE than in AAH and higher in AD than in AAH ($P < 0.05$, respectively) (Fig. 2a). In contrast, the LI of Ki-67, immunoreactivity of which was observed in the nuclei of the cells (Fig. 1f), was lower in BE than in AAH and lower in AAH than in AD ($P < 0.05$, respectively) (Fig. 2b).

When we compared the P27 LI and the Ki-67 LI with high Skp2 or Jab1 expression (Table 2), high Skp2 or Jab1 expression was significantly correlated to a lower P27 LI. No interaction of Skp2 and Jab1 concerning the P27 labeling index was confirmed by variance analysis (F-value, 3.03; P-value, 0.08). For the Ki-67 LI, high Skp2 or Jab1 expression was significantly correlated to a higher Ki-67 LI. We also analyzed the relationship between P27 expression and the Ki-67 LI. Low P27 expression (Ki-67 LI = 15) did not show a significantly higher Ki-67 LI than high P27 expression (Ki-67 LI = 11).

Correlation between high Skp2 and Jab1 expressions and clinicopathological factors in lung adenocarcinoma

The data are summarized in Table 3, with those of P27 and Ki-67. Blood and lymphatic vessel invasion significantly correlated with Skp2 overexpression ($P = 0.002$ and $P = 0.003$, respectively).

Prognostic significance of Skp2 and Jab1 overexpression in lung adenocarcinoma

The prognostic significance of Skp2 and Jab1 overexpression was analyzed using the Kaplan–Meier method in lung AD, together with analysis of the P27 and Ki-67 LI (Fig. 3a–d). The patients with Skp2-high or P27-low carcinoma showed a significantly worse outcome compared with those with Skp2-low or P27-high carcinomas, respectively. Jab1-high or Ki-67-low lung AD did not differ with statistical significance from Jab1-low or Ki-67-low cases in the clinical outcome.

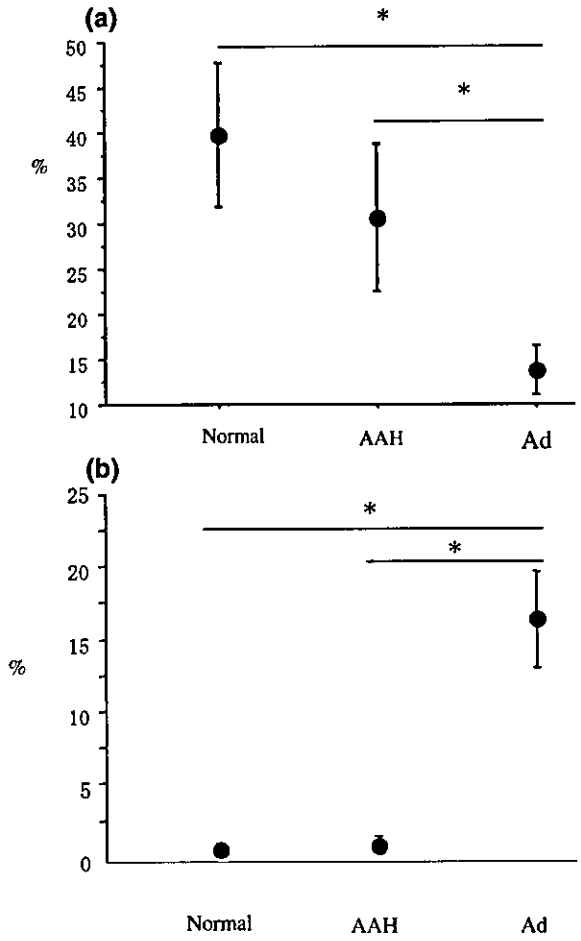

Figure 2 P27 and Ki-67 labeling indexes in lung bronchiolar epithelium, atypical adenomatous hyperplasia (AAH) and adenocarcinoma (Ad). Each point and bar indicates the mean ± 95% confidence interval in the subgroups. (**a**) Mean labeling index of P27. (**b**) Mean labeling index of Ki-67. *$P < 0.05$.

Table 2 Correlations between high Skp2 or Jab1 expression and P27 or Ki-67 labeling index in lung bronchiolar epithelium, AAH and adenocarcinoma

	P27 LI (%)	Ki-67 LI (%)
Skp2		
High expression	14	22
Low expression	20 *	7 *
Jab1		
High expression	12	17
Low expression	23 *	10 *

AAH, atypical adenomatous hyperplasia. LI, labeling index. *$P < 0.05$.

Table 3 High Skp2, Jab1, Ki-67 or low P27 immunoreactivity and clinicopathological factors in lung adenocarcinoma

	n	High Skp2 (%)	High Jab1 (%)	High Ki-67 (%)	Low P27 (%)
Histological differentiation					
Well	56	32 (49)	30 (48)	7 (13)	24 (43)
Moderately and poorly	54	20 (44)	29 (78)	20 (37)	45 (83)
Lymph node metastasis					
+	45	25 (44)	27 (41)	10 (22)	28 (62)
–	65	27 (50)	32 (49)	17 (26)	41 (63)
Lymphatic vessel invasion					
+	86	47 (55)*	44 (51)	20 (23)	56 (65)
–	24	5 (21)*	15 (63)	7 (29)	13 (54)
Blood vessel invasion					
+	87	46 (53)*	48 (55)	23 (26)	58 (67)
–	23	6 (27)*	11 (48)	4 (17)	11 (48)
Pleural infiltration					
+	63	32 (51)	33 (52)	18 (29)	36 (57)
–	47	20 (43)	26 (55)	9 (19)	33 (70)
Pleural dissemination					
+	13	5 (38)	7 (54)	3 (23)	10 (77)
–	97	47 (48)	52 (54)	24 (25)	59 (59)
Intrapulmonary metastasis					
+	11	6 (55)	7 (64)	2 (18)	7 (64)
–	99	46 (46)	52 (53)	25 (25)	62 (63)
Stage					
I and II	59	21 (36)	33 (56)	7 (11)	38 (64)
III and IV	51	31 (61)	26 (51)	20 (39)	32 (63)

–, Absent; +, present. *$P < 0.05$.

We also analyzed the prognostic significance of Skp2 in the cases of P27-high AD and P27-low AD, respectively. Although the differences were not statistically significant, Skp2-high AD showed a relatively worse outcome than Skp2-low AD (Fig. 4a,b).

DISCUSSION

Skp2 and Jab1 are two key molecules in the degradation of P27.[9–12] Inverse correlation between Skp2 or Jab1 and P27 has been observed in various neoplasms.[13–18] In the present study, we confirmed that P27 expression decreased in AD of the lung, and that its considerable decrease was a prognostic determinant of lung AD. Therefore, reciprocal expression of each molecule against P27 in the present study suggests that overexpression of Skp2 or Jab1 is certainly involved in the tumorigenesis of lung AD, through down-regulation of P27. However, to date, there has been no study that concurrently examined abnormalities of these two proteins on the same clinical specimens. In the present study of lung AD, we confirmed that there was no interaction of Skp2 or Jab1 overexpression concerning the P27 labeling index by variance analysis. Thus, these two proteins might play a different or independent role in the degradation process of P27, and overexpression of either molecule might lead to the decrease of P27 expression in lung AD.

Various studies investigating P53 protein overexpression, K-ras gene mutation and clonality have suggested that AAH is a putative precancerous lesion of lung AD.[19] In the present study, overexpression of Jab1 was observed in some AAH. However, the labeling index of P27 or Ki-67 was not significantly decreased or increased compared with the normal bronchiolar epithelium. Jab1 antagonizes TGF-beta signaling by inducing Smad4 degradation and stabilizing hypoxia induced factor (HIF)-1 alpha by direct interaction.[23,24] These properties of Jab1 are not mediated by P27, and might be associated with the early phase of development of AAH.

For the Ki-67 LI, high Skp2 or Jab1 expression was significantly correlated to a higher Ki-67 LI. However, low P27 expression did not correlate to a higher Ki-67 LI in the present study. This suggests that an increase in the Ki-67 LI is not determined solely or directly by the loss of P27 expression, and functional loss of other cell-cycle inhibitory proteins such as P16 might cooperate with the decrease of P27, or high expression of Skp2 and Jab1 might increase the Ki-67 LI through P27-independent mechanisms.[4]

The prognostic significance of Skp2 overexpression was demonstrated in gastric cancer and diffuse large B-cell lymphoma.[15,16] Concerning tumor aggressiveness, Masuda *et al.* demonstrated an increase of invasion potential of Skp2 transfected gastric cancer cells, which were regulated by Rho family GTPases (Rho, Rac and Cdc42) and suggested P27 unmediated contribution of Skp2 for tumor progression.[15,25] The prognostic significance of loss of P27 expression was also reported in various cancers including non-small cell lung cancer and gastric cancer.[5,26,27] In the present study, we demonstrated that overexpression of Skp2 and a considerable decrease of P27 were prognostic determinants in lung AD. In contrast, Jab1 overexpression failed to correlate to any of

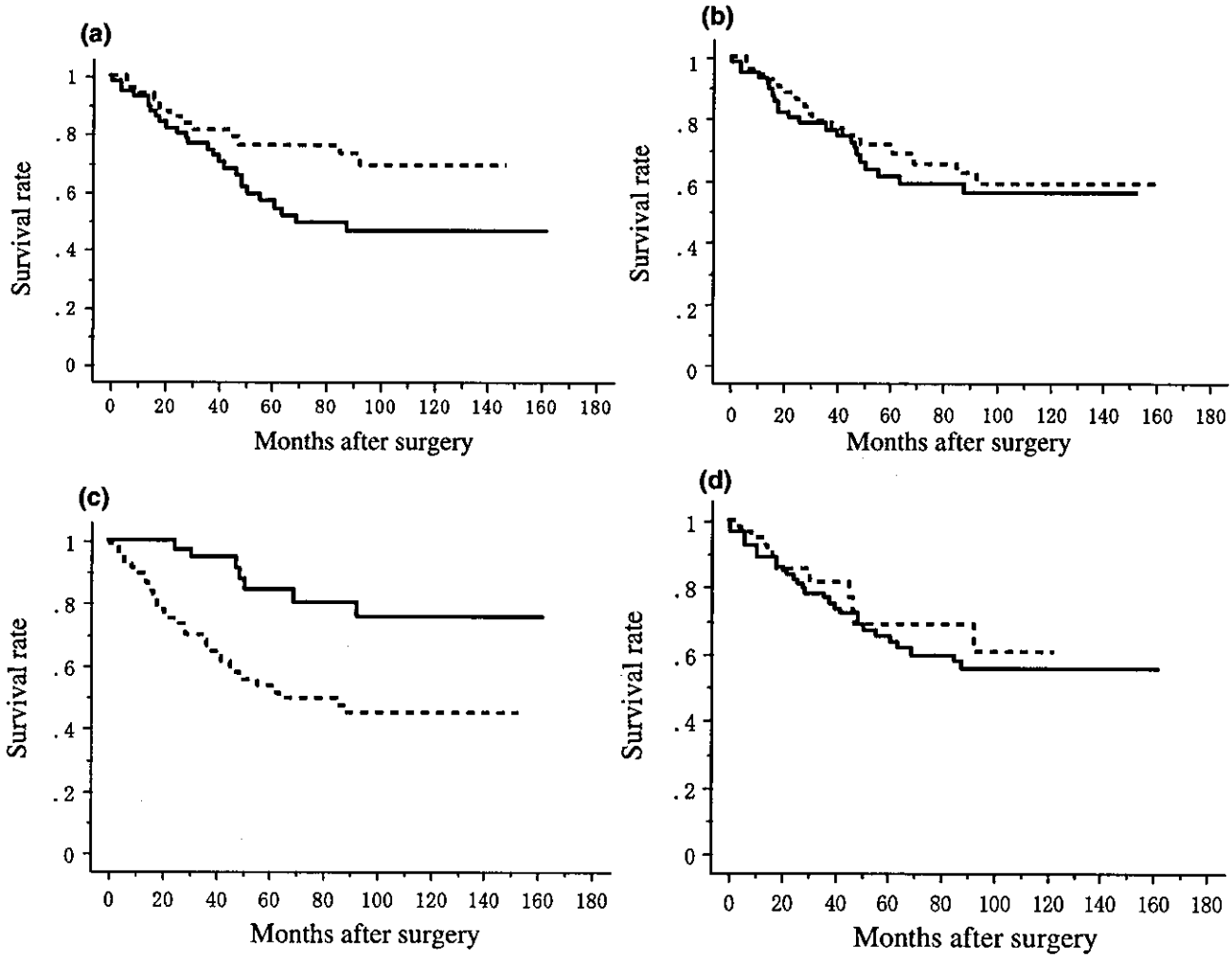

Figure 3 Kaplan–Meier survival curves of lung adenocarcinoma cases. Survival curves were stratified in terms of (**a**) Skp2, (**b**) Jab1, (**c**) P27 and (**d**) Ki-67. (- - -), Low; (—), High.

the clinicopathological factors and Jab1-high cases did not show a worse prognosis than Jab1-low cases in the present study. As the overexpression of both proteins reciprocally correlated with P27 in an independent manner, the worse prognosis of Skp2-high AD cases was not solely explained on the basis of augmentation of P27 degradation. In fact, the present study showed that Skp2 overexpression was correlated with vascular and lymphatic invasion, which low P27 expression did not correlate with. Furthermore, Skp2-high cases showed a relatively worse clinical outcome, even in the P27-high AD cases. This also suggests a P27 unmediated contribution of Skp2 for the progression of lung Ad, as observed in Skp2-transfected gastric cancer cells.

In conclusion, overexpression of Skp2 and Jab1 was frequently observed in lung AD, which correlated with a decrease in P27 expression, suggesting the importance of both degradation pathways of P27 in lung AD. Overexpression of both molecules might play a role in the acceleration of the proliferative activity in AD through P27-dependent and P27-independent mechanisms. Skp2 overexpression was associated with vascular and lymphatic invasion and indicative of a poor prognosis for the patients with lung AD. Further investigations are needed to elucidate the mechanism on how Skp2 or Jab1 is overexpressed and how overexpression of Skp2 influences patient's survival in lung AD.

ACKNOWLEDGMENTS

This study was supported in part by a grant from Nishi Cancer Research Fund, the Vehicle Racing Commemorative Foundation, Ministry of Health, Labour and Welfare of Japan, and Grant-in-Aid for Scientific Research on Priority Areas from the Ministry of Education, Culture, Sports, Science and Technology of Japan. The authors wish to thank A. Harada and M. Saito for their excellent technical assistance.

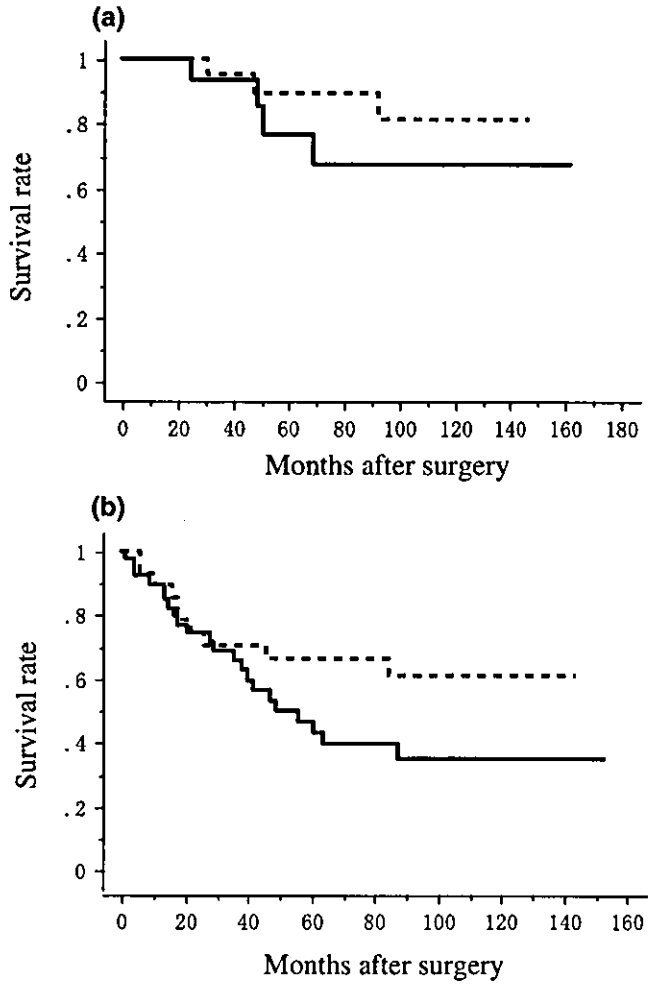

Figure 4 Kaplan–Meier survival curves of (a) P27-high and (b) P27-low lung adenocarcinoma cases. Survival curves were stratified in terms of Skp2. (- - -), Skp2-low; (—), Skp2-high.

REFERENCES

1 Gupta AK, Harris EER, Bernhard EJ *et al.* Overview of cell cycle and apoptosis. In: Pass HI, Mitchell JB, Johnson DH, Turrisi AT, Minna JD, eds. *Lung Cancer Principles and Practice.* Philadelphia: Lippincott Williams & Wilkins, 2000; 5–67.

2 Forgacs E, Zochbauer-Muller S, Olah E, Minna JD. Molecular genetic abnormalities in the pathogenesis of human lung cancer. *Pathol Oncol Res* 2001; **7**: 6–13.

3 Dobashi Y, Shoji M, Jiang SX, Kobayashi M, Kawakubo Y, Kameya T. Active cyclin A-CDK2 complex, a possible critical factor for cell proliferation in human primary lung carcinomas. *Am J Pathol* 1998; **153**: 963–72.

4 Kawabuchi B, Moriyama S, Hironaka M *et al.* p16 inactivation in small-sized lung adenocarcinoma: its association with poor prognosis. *Int J Cancer* 1999; **84**: 49–53.

5 Esposito V, Baldi A, De Luca A *et al.* Prognostic role of the cyclin-dependent kinase inhibitor p27 in non-small cell lung cancer. *Cancer Res* 1997; **57**: 3381–5.

6 Hayashi H, Ito T, Yazawa T *et al.* Reduced expression of p27/Kip1 is associated with the development of pulmonary adenocarcinoma. *J Pathol* 2000; **192**: 26–31.

7 Toyoshima H, Hunter T. p27, a novel inhibitor of G1 cyclin-Cdk protein kinase activity, is related to p21. *Cell* 1994; **78**: 67–74.

8 Kawamata N, Morosetti R, Miller CW *et al.* Molecular analysis of the cyclin-dependent kinase inhibitor gene p27/Kip1 in human malignancies. *Cancer Res* 1995; **55**: 2266–9.

9 Carrano AC, Eytan E, Hershko A, Pagano M. SKP2 is required for ubiquitin-mediated degradation of the CDK inhibitor p27. *Nat Cell Biol* 1999; **1**: 193–9.

10 Sutterluty H, Chatelain E, Marti A *et al.* p45SKP2 promotes p27Kip1 degradation and induces S phase in quiescent cells. *Nat Cell Biol* 1999; **1**: 207–14.

11 Tomoda K, Kubota Y, Kato J. Degradation of the cyclin-dependent-kinase inhibitor p27Kip1 is instigated by Jab1. *Nature* 1999; **398**: 160–65.

12 Tomoda K, Kubota Y, Arata Y *et al.* The cytoplasmic shuttling and subsequent degradation of p27Kip1 mediated by Jab1/CSN5 and the COP9 signalosome complex. *J Biol Chem* 2002; **277**: 2302–10.

13 Yokoi S, Yasui K, Saito-Ohara F *et al.* A novel target gene, SKP2, within the 5p13 amplicon that is frequently detected in small cell lung cancers. *Am J Pathol* 2002; **161**: 207–16.

14 Gstaiger M, Jordan R, Lim M *et al.* Skp2 is oncogenic and overexpressed in human cancers. *Proc Natl Acad Sci USA* 2001; **98**: 5043–8.

15 Masuda TA, Inoue H, Sonoda H *et al.* Clinical and biological significance of S-phase kinase-associated protein 2 (Skp2) gene expression in gastric carcinoma: modulation of malignant phenotype by Skp2 overexpression, possibly via p27 proteolysis. *Cancer Res* 2002; **62**: 3819–25.

16 Seki R, Okamura T, Koga H *et al.* Prognostic significance of the F-box protein Skp2 expression in diffuse large B-cell lymphoma. *Am J Hematol* 2003; **73**: 230–35.

17 Tsuchida R, Miyauchi J, Shen L *et al.* Expression of cyclin-dependent kinase inhibitor p27/Kip1 and AP-1 coactivator p38/Jab1 correlates with differentiation of embryonal rhabdomyosarcoma. *Jpn J Cancer Res* 2002; **93**: 1000–6.

18 Kouvaraki MA, Rassidakis GZ, Tian L, Kumar R, Kittas C, Claret FX. Jun activation domain-binding protein 1 expression in breast cancer inversely correlates with the cell cycle inhibitor p27 (Kip1). *Cancer Res* 2003; **63**: 2977–81.

19 Kitamura H, Kameda Y, Ito T, Hayashi H. Atypical adenomatous hyperplasia of the lung. Implications for the pathogenesis of peripheral lung adenocarcinoma. *Am J Clin Pathol* 1999; **111**: 610–22.

20 Mountain CF. Revisions in the International System for Staging Lung Cancer. *Chest* 1997; **111**: 1710–17.

21 The Japan Lung Cancer Society. *General Rule for Clinical and Pathological Record of Lung Cancer.* Tokyo, Japan: Kanehara & Co., Ltd; 1999.

22 Luk C, Tsao MS, Bayani J, Shepherd F, Squire JA. Molecular cytogenetic analysis of non-small cell lung carcinoma by spectral karyotyping and comparative genomic hybridization. *Cancer Genet Cytogenet* 2001; **125**: 87–99.

23 Wan M, Cao X, Wu Y *et al.* Jab1 antagonizes TGF-beta signaling by inducing Smad4 degradation. *EMBO Rep* 2002; **3**: 171–6.

24 Bae MK, Ahn MY, Jeong JW *et al.* Jab1 interacts directly with HIF-1alpha and regulates its stability. *J Biol Chem* 2002; **277**: 9–12.

25 Hall A. Rho GTPases and the actin cytoskeleton. *Science* 1998; **279**: 1998.

26 Mori M, Mimori K, Shiraishi T *et al.* P27 expression and gastric carcinoma. *Nat Med* 1997; **3**: 593.

27 Slingerland J, Pagano M. Regulation of the cdk inhibitor p27 and its deregulation in cancer. *J Cell Physiol* 2000; **183**: 10–17.